RECENT MEASUREMENT OF THE ZGS INJECTOR BEAM CHARACTERISTICS*

E. F. Parker
Argonne National Laboratory
Argonne, Illinois

Abstract

Detailed measurements of the energy, energy spread and emittance as a function of time, rf level, preaccelerator high voltage and linac-debuncher relative phase have been made using a series of segmented faraday cups recently installed in the Zero Gradient Synchrotron (ZGS). A strong energy dependence upon rf level and preaccelerator high voltage which has significant implications for the ZGS is found.

Introduction

As a result of the installation of a new diagnostic system in the ZGS, the characteristics of the injector beam can be examined to a level of detail never before possible. Using the ZGS as a spectrometer and a new detector system, the energy spread, emittance, and energy changes of the injector beam can be measured as a function of time during the beam pulse.

The new detector system consists of a series of four segmented faraday cups (SFC) located around the ZGS as shown in Fig. 1. The L-1 SFC consists of both a vertical and horizontal array located at the downstream end of the inflector. Each array consists of thirty-six 0.08 cm-wide detectors, separated by 0.11 cm. These two SFC give the profile and position of the beam in both planes as it is injected into the ZGS. The L-2 SFC is a vertical array of thirty-six 0.16 cm-wide detectors extending across the vertical aperture of the ZGS. Since L-2 is approximately 90° away from the inflector in betatron space, this array measures the vertical divergence of the beam. The L-3 SFC is a horizontal array of forty-two 0.95 cm wide detectors extending across the horizontal aperture of the ZGS. Located approximately 180° away from the inflector in betatron space, this detector measures the energy (relative) and energy spread of the injected beam. This detector is partially transparent so some of the beam survives to hit this detector on the next turn which corresponds to a position approximately 90° away from the inflector. This allows a measurement of the horizontal divergence of the injector beam. The third turn can also be seen on the L-3 SFC and this allows a determination of the injection angle. Figure 2 is a photograph of the L-3 SFC. Figure 3 is a schematic of the electronics used with these SFC. The front end transistors act as a fast double throw switch which allows the detectors to be simultaneously activated for as little as 5 μsec, thereby allowing snapshots of the beam to be taken at any time during the beam pulse. The outputs of the detectors are read into the MCR computer and displayed on a CRT. Further engineering and physics detail about this system are not appropriate here but will be the subject of several papers to be submitted to the 1973 Particle Accelerator Conference. The purpose of this report is to present data on the characteristics of the ZGS injector beam obtained to date with this system.

Results

Figure 4 shows the mean energy, energy spread, and horizontal emittance of the injector beam vs. linac rf level. Since only energy changes can be measured, the energy scale is normalized to the energy at rf = 1.155 V. The emittance is obtained by measuring the size and divergence of the beam as it exits the inflector. These data therefore actually give the area of the x, x' box which contains the injected beam and is therefore an upper limit of the actual area, equaling the area if the ellipse is upright (as should be the case to a good approximation). Also, since a small fraction of the beam is lost in the transport line between the linac and the achromats, only 90-95% of the beam is included. At rf levels below 1.12 V, the energy spread was too large to be contained (>1 MeV). These data were taken with normal beam (approximately 38 mA) and the ALC adjusted to provide a constant rf level during the pulse. Each reading was taken at exactly the same point in the pulse. At rf levels above 1.165 V, the energy distribution of the beam breaks up into two distinct peaks, one at approximately the nominal energy containing approximately 75% of the beam. The three energy points plotted in Fig. 4 for the two highest rf level settings correspond to the mean energy of each peak and the mean energy of the total distribution. The rapid fall-off in energy with rf is similar to or perhaps a bit more severe than that found by others.[1, 2, 3] Whether or not this is due simply to a bad gradient tilt has not yet been experimentally investigated. A -20% tilt presently exists in the ZGS injector. The vertical emittance was not measured at each rf level but every place it was checked yielded a value slightly higher than the radial value, i.e. approximately $0.7 \pm .1\pi$ mr-in. The error bars indicate the estimated precision of the measurements. The line through the energy points is just to guide the eye. The line through the emittance data is the average value of the data. The line through the energy spread data is a sine fit.

Figure 5 shows the mean energy during the 200-μsec beam pulse when the rf is approximately constant at about 1.15 V. Curve (a) was taken with

*Work performed under the auspices of the U. S. Atomic Energy Commission

the ALC gain set as low as possible while still holding the rf approximately constant. Under this condition, the rf level is "smooth" during the last 70% of the beam pulse. Curve (b) was taken with the ALC gain at its "normal" level. Under this condition, the pickup loop on the linac tank shows a low level 30-kc oscillation during the beam pulse. Except for the energy variation due to the slight rf ramp, curve (a) shows the energy to be constant during the pulse when the oscillations are not present. Curve (b) shows that the oscillations modulate the output energy as expected from Fig. 4. These oscillations are attributed to moding in the tank during filling. Because of the inherent time delay in the ALC system, the ALC at high gain causes them to persist throughout the pulse. The energy spread is constant across the pulse.

Figure 6 shows the energy distribution as a function of preaccelerator voltage. The buncher and 750-keV transport beam parameters were held constant. A ΔV of 6 kV corresponds to a 54° phase shift of the beam bunch at the first linac gap. Although the energy spread remains constant, most of the beam shifts to the high energy side of the distribution as the voltage decreases. At a preaccelerator voltage of approximately 710 kV, which corresponds to a phase shift of one rf cycle, the normal energy profile is once again obtained [curve (a) in Fig. 6].

Figure 7 shows the energy and energy spread of the beam as a function of debuncher-linac relative phase. The solid lines are sine and cosine fits to the energy and energy spread data respectively. The debuncher is used only as a diagnostic aid at the ZGS. These data are included primarily as a graphic display of the capabilities of this new detector system.

For machines requiring short injector pulses or which have a large momentum compaction factor, the energy variations presented above are of little practical importance. At the ZGS, however, this is not the case. When the highest accelerated intensities are obtained, the injector is tuned so that the rf gradient is ramped up about 3% and the preaccelerator voltage is ramped down by about 4 kV during the 200-μsec beam pulse. Injection timing is critical down to the 10-μsec level even though the injector pulse is almost twice as long as the acceptance time of the ZGS. The data presented in Figs. 4 and 6 make it clear now why these strange conditions work best. The net result of the mean energy ramping up with the rf and the shift of most of the beam to the high energy side of the distribution due to the preaccelerator voltage ramping down is $dE/dt = 2.1$ keV/μsec during the pulse. This keeps the betatron oscillation amplitudes small at the expense of energy spread. A $dE/dt = 3.7$ keV/μsec is required to exactly counteract the normal 17.5 kG/sec magnetic field ramp used at the ZGS. Programming the ZGS linac rf to provide ramped energy injection was suggested some years ago[4] but was never deliberately attempted. It now turns out that, in fact, it was tried by accident and seems to work quite well.

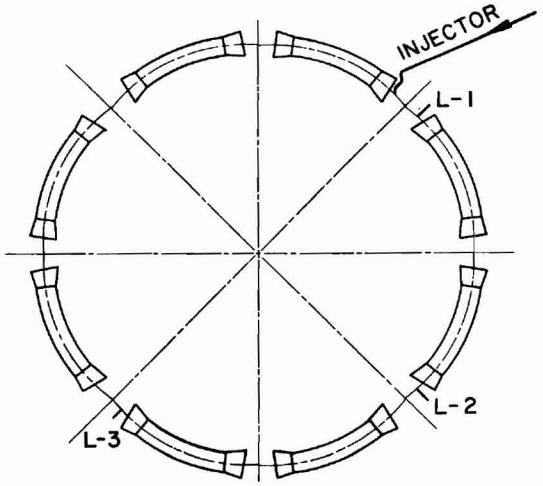

Fig. 1 Segmented Faraday cup locations

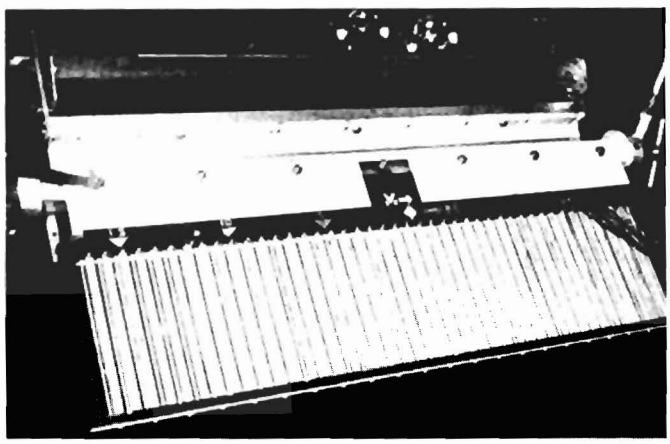
Fig. 2 L-3 segmented Faraday cup

References

[1] K. Batchelor, R. Chasman, and T. Werntz, "Measurements and Calculations on the 50-MeV Brookhaven Linac," Proceedings of the 1966 Linear Accelerator Conference, LA-3609, p. 28 (1966).

[2] K. Batchelor, "Beam Observation in the P. L. A.," Minutes of Conference on Linear Accelerators for High Energies, BNL 6511, p. 235 (1962).

[3] R. W. Allison, D. M. Evens, R. M. Richter, A. J. Sherwood, and E. Zajec, "Measurements of the Linear-Accelerator Exit Beam of the Bevatron Injector," Proceedings of the 1966 Linear Accelerator Conference, LA-3609, p. 34 (1966).

[4] P. V. Livdahl, "ZGS Injector Observations," Minutes of the 1964 Conference on Proton Linear Accelerators, MURA 714, p. 384 (1964).

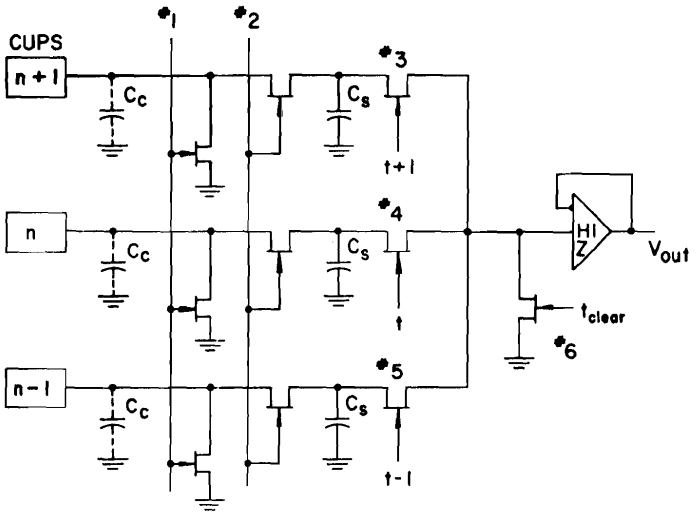

Fig. 3 Segmented Faraday cup electronics

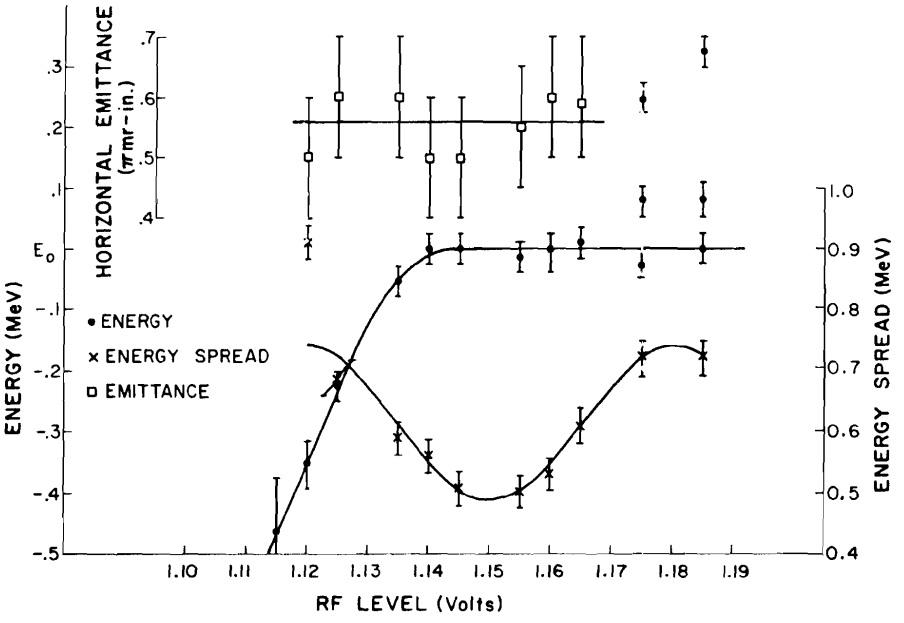

Fig. 4 Energy, energy spread, and emittance vs linac rf level

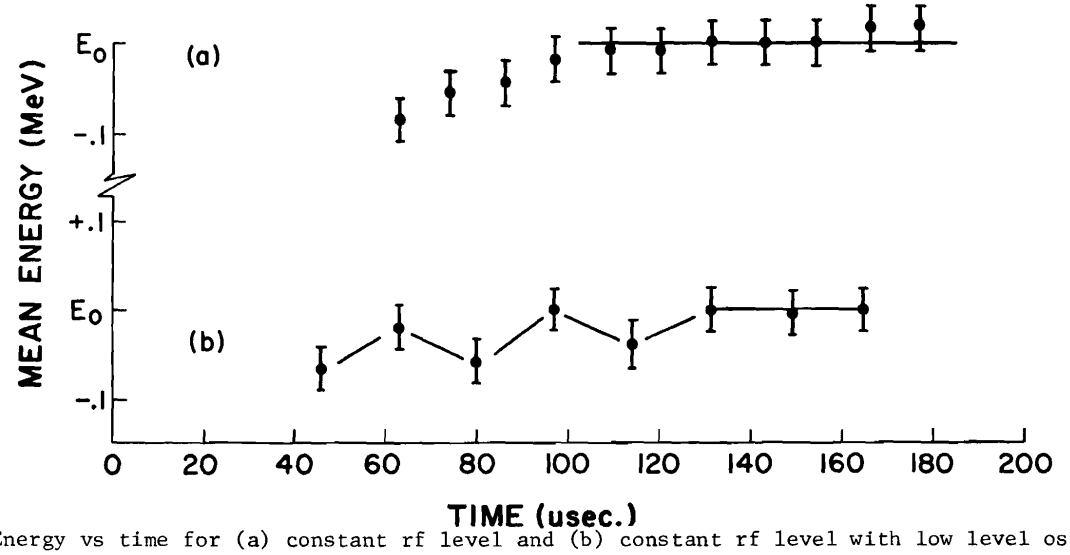

Fig. 5 Energy vs time for (a) constant rf level and (b) constant rf level with low level oscillation

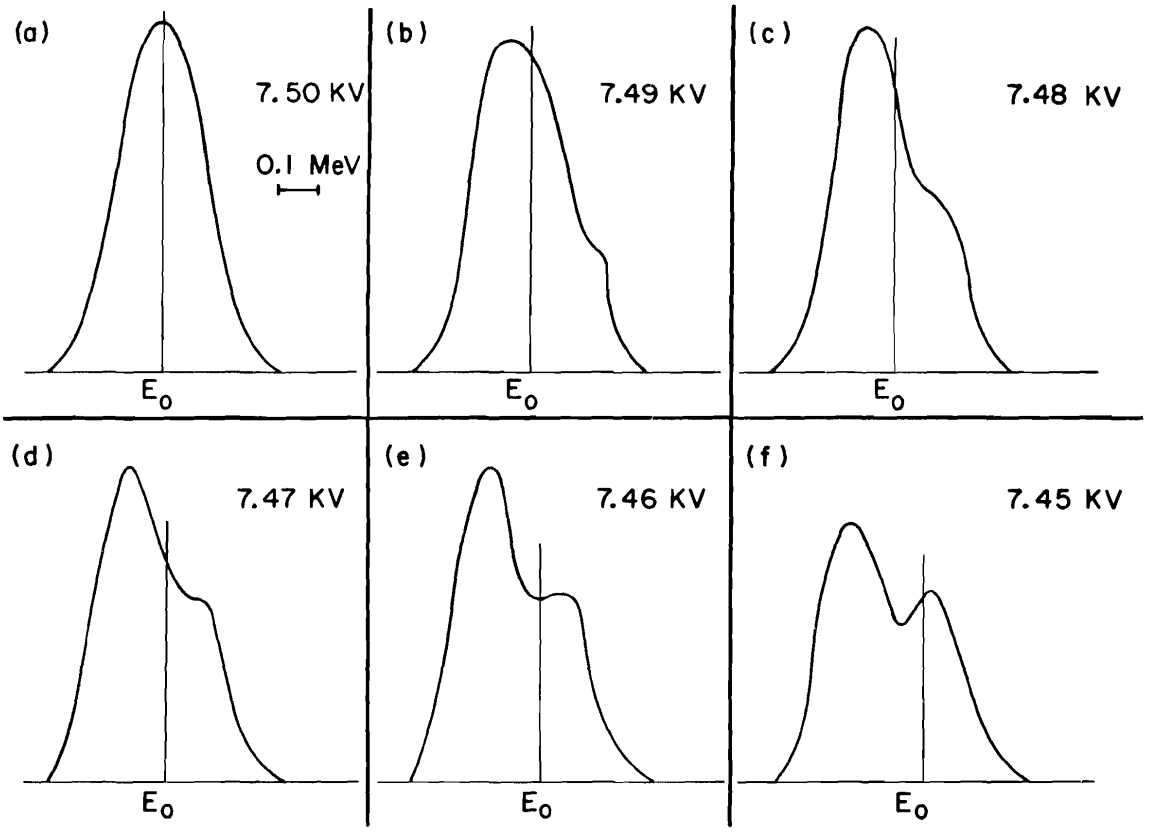

Fig. 6 Output energy distribution vs preaccelerator high voltage

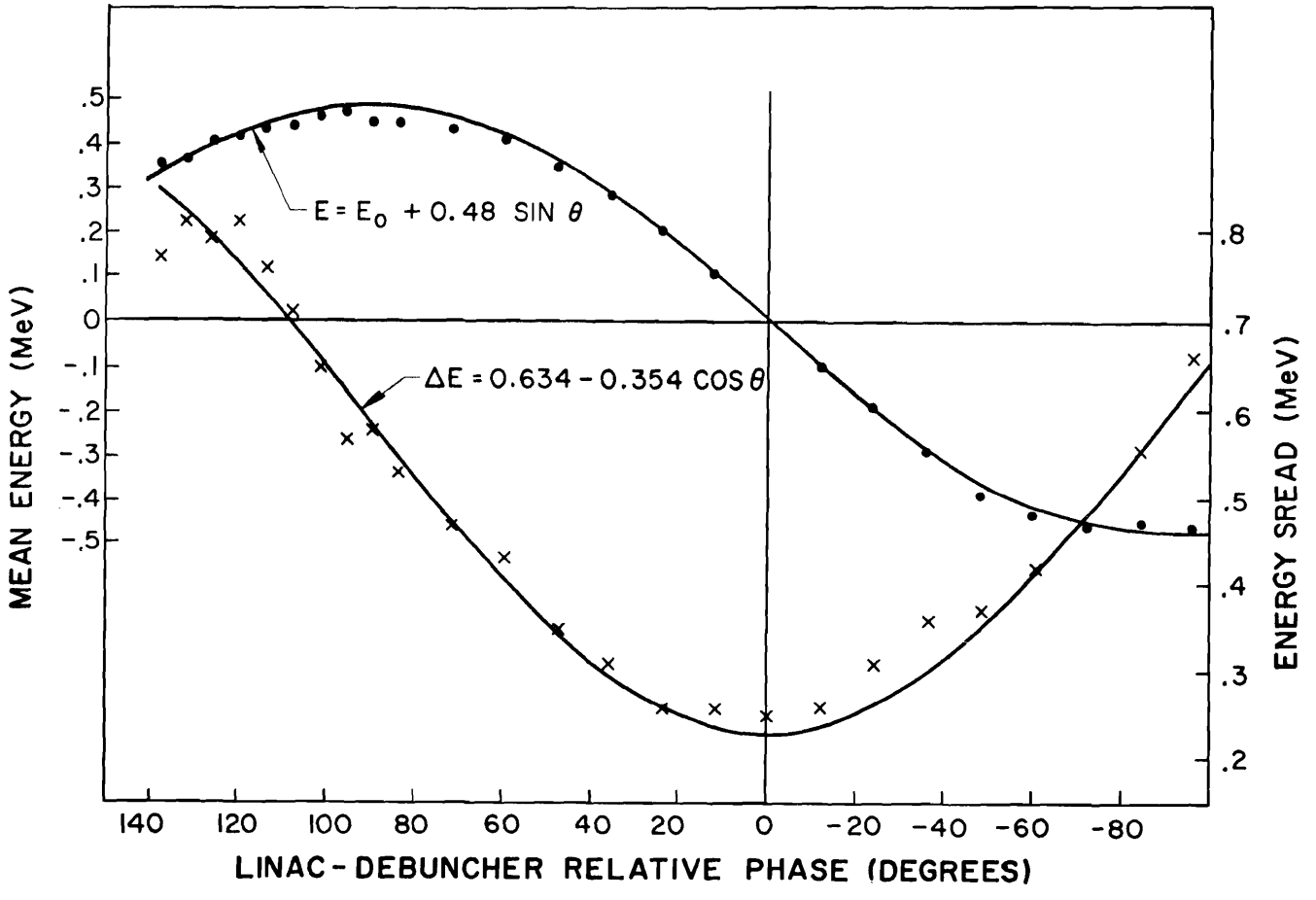

Fig. 7 Energy and energy spread vs linac-debuncher relative phase